

Transient Magnetohydrodynamic Free Convective Heat and Mass Transfer Flow with Thermophoresis past a Radiate Inclined Permeable Plate in the Presence of Variable Chemical Reaction and Temperature Dependent Viscosity

M. S. Alam^{1*}, M. M. Rahman¹, M. A. Sattar²

¹Department of Mathematics, University of Dhaka, Dhaka-1000, Bangladesh
mansurdu@yahoo.com

²Department of Computer Science and Engineering, North South University
12 Kemal Ataturk Avenue, Banani, Dhaka-1213, Bangladesh

Received: 2008-03-09 **Revised:** 2008-09-08 **Published online:** 2009-03-10

Abstract. In the present study, an analysis is carried out to investigate the effects of variable chemical reaction, thermophoresis, temperature-dependent viscosity and thermal radiation on an unsteady MHD free convective heat and mass transfer flow of a viscous, incompressible, electrically conducting fluid past an impulsively started infinite inclined porous plate. The governing nonlinear partial differential equations are transformed into a system of ordinary differential equations, which are solved numerically using a sixth-order Runge-Kutta integration scheme with Nachtsheim-Swigert shooting method. Numerical results for the non-dimensional velocity, temperature and concentration profiles as well as the local skin-friction coefficient, the local Nusselt number and the local Stanton number are presented for different physical parameters. The results show that variable viscosity significantly increases viscous drag and rate of heat transfer. The results also show that higher order chemical reaction induces the concentration of the particles for a destructive reaction and reduces for a generative reaction.

Keywords: variable viscosity, chemical reaction, thermophoresis, unsteady flow, thermal radiation.

1 Introduction

Prediction of particle transport in non-isothermal gas flow is important in studying the erosion process in combustors and heat exchangers, the particle behavior in dust collectors, and the fabrication of optical waveguide and semiconductor device, and so on.

*Permanent address: Department of Mathematics, Dhaka University of Engineering and Technology (DUET), Gazipur-1700, Bangladesh.

Environmental regulations on small particles have also become more stringent due to concerns about atmospheric pollution.

When a temperature gradient is established in gas, small particles suspended in the gas migrate in the direction of decreasing temperature. This phenomenon, called thermophoresis, occurs because gas molecules colliding on one side of a particle have different average velocities from those on the other side due to the temperature gradient. Hence, when a cold wall is placed in the hot particle-laden gas flow, the thermophoretic force may cause particles to be deposited on it. The magnitude of this force depends on gas and particle properties as well as on the temperature gradient. The thermophoretic deposition plays an important role in a variety of applications such as the production of ceramic powders in high temperature aerosol flow reactors; the production of optical fiber preforms by the modified chemical vapor deposition (MCVD) process and in polymer separation. Thermophoresis is considered to be important for particles of 10 nm in radius and temperature gradient of the order of 5K/mm. Walker et al. [1] calculated the deposition efficiency of small particles due to thermophoresis in a laminar tube flow. The effect of wall suction and thermophoresis on aerosol-particle deposition from a laminar boundary layer on a flat plate was studied by Mills et al. [2]. Ye et al. [3] analyzed the thermophoretic effect of particle deposition on a free standing semiconductor wafer in a clean room. Thakurta et al. [4] computed numerically the deposition rate of small particles on the wall of a turbulent channel flow using the direct numerical simulation (DNS). Cluster transport and deposition processes under the effects of thermophoresis were investigated numerically in terms of thermal plasma deposition processes by Han and Yoshida [5]. In their analysis, they found that the thickness of the concentration boundary layer was significantly suppressed by the thermophoretic force and it was concluded that the effect of thermophoresis plays a more dominant role than that of diffusion. Recently, Alam et al. [6] investigated numerically the effect of thermophoresis on surface deposition flux on hydromagnetic free convective heat and mass transfer flow along a semi-infinite permeable inclined flat plate considering heat generation. Their results show that thermophoresis increases surface mass flux significantly.

The previous studies, dealt with thermophoresis, neglected the effect of thermal radiation. But in fact, there are various kinds of high temperature systems such as a heat exchanger and an internal combustor, in which the radiation may not be negligible in comparison with the conductive and convective heat transfer mode. Usually, the gas like CO₂ and H₂O generated during combustion of a hydrocarbon fuel and the particles such as soot and coal suspended in a hot gas flow absorb, emit and scatter the radiation. In light of this importance, Yoa et al. [7] investigated numerically the thermophoresis phenomenon in a laminar tube flow by taking into account the particle radiation. The radiation effect on the thermophoresis of particles was analyzed for a gas-particle two-phase laminar flow by Sohn et al. [8]. Akbar and Ghiaasiaan [9] studied numerically the combined effects of radiation heat transfer and thermophoresis on the transport of monodisperse, as well as polydisperse soot particles. Recently, Alam et al. [10] experiments numerically the thermal radiation interaction of thermophoresis on free-forced convective heat and mass transfer flow along a semi-infinite permeable inclined flat plate. Their results show that interaction of thermal radiation with thermophoresis depositing

surface mass flux is significant. Very recently Cortell [11–13] investigated theoretically the effects of viscous dissipation as well as radiation on the thermal boundary layer flows over nonlinearly stretching sheets considering prescribed surface temperature and heat flux.

However in convective heat and mass transfer process, diffusion rates can be altered tremendously by chemical reaction. The effect of a chemical reaction depends on whether the reaction is heterogeneous or homogeneous. This also depends on whether they occur at an interface or as a single phase volume reaction. A reaction is said to be of the order n , if the reaction rate is proportional to the n -th power of the concentration. In particular, a reaction is said to be first order, if the rate of the reaction is directly proportional to the concentration itself. In nature, the presence of pure air or water is not possible. Some foreign mass may be present either naturally or mixed with the air or water. The presence of a foreign mass in air or water causes some kind of chemical reaction. The study of such type of chemical reaction processes is useful for improving a number of chemical technologies, such as food processing and polymer production. Chambre and Young [14] analyzed the problem of first order chemical reactions in the neighborhood of a flat plate for destructive and generative reactions. Das et al. [15] studied the effect of homogeneous first order chemical reaction on the flow past an impulsively started infinite vertical plate with uniform heat flux and mass transfer. Anjalidevi and Kandasamy [16] analyzed the effect of a chemical reaction on the flow in the presence of heat transfer and magnetic field. Muthucumaraswamy and Ganesan [17] studied the effect of a chemical reaction on an unsteady flow past an impulsively started vertical plate which is subjected to uniform mass flux and in the presence of heat transfer. Raptis and Perdikis [18] studied numerically the steady two-dimensional flow of an incompressible viscous and electrically conducting fluid over a non-linearly semi-infinite stretching sheet in the presence of a chemical reaction and under the influence of a magnetic field. Cortell [19, 20] studied MHD heat and mass transfer flow of second grade fluids over nonlinearly stretching sheet with chemically reactive species in a porous medium. Recently, Alam et al. [21] investigated the effects of thermophoresis and first order chemical reaction on unsteady hydromagnetic free convection and mass transfer flow past an impulsively started infinite inclined porous plate in the presence of heat generation/absorption.

Most of the above studies are based on the constant physical properties of the ambient fluid. However, it is known that these properties may change with temperature, especially fluid viscosity. To predict accurately the flow behavior and heat transfer rate, it is necessary to take this variation of viscosity into account. In view of this importance, Kafoussias and Williams [22] studied the thermal diffusion and diffusion thermo effects on mixed free-forced convective mass transfer boundary layer flow with temperature dependent viscosity. Seddeek [23] studied the effect of variable viscosity on hydrodynamic flow and heat transfer past a continuously moving porous boundary with radiation. Very recently, Molla and Hossain [24] investigated the effects of chemical reaction, heat and mass diffusion in natural convection flow from an isothermal sphere with temperature-dependent viscosity.

Therefore the objective of the present paper is to investigate the effects of higher order chemical reaction and thermophoresis on an unsteady MHD free convective heat

and mass transfer flow past an impulsively started infinite inclined porous plate in the presence of thermal radiation with temperature-dependent viscosity.

2 Mathematical formulation

We consider an unsteady MHD free convective heat and mass transfer flow of an electrically conducting (for examples plasmas, liquid metals, salt water, air etc) incompressible viscous fluid past an infinite inclined porous flat plate with an acute angle α to the vertical. The flow is assumed to be in the x -direction, which is taken along the inclined plate and y -axis normal to it. A magnetic field of uniform strength B_0 is introduced normal to the direction of the flow. Initially ($t = 0$) the plate and the fluid are at rest. But for time $t > 0$, the plate starts moving impulsively in its own plane with a velocity U_0 , its temperature is raised to T_w which is higher than the ambient temperature T_∞ . The species concentration at the surface is maintained uniform at C_w , which is taken to be zero and that of the ambient fluid is assumed to be C_∞ . Fluid suction or injection is imposed at the plate surface. In addition, the effect of thermophoresis is taken into account as it helps in understanding mass deposition on surface. We further assume that (i) the magnetic Reynolds number is assumed to be small so that the induced magnetic field is negligible in comparison to the applied magnetic field, (ii) due to the boundary layer behavior the temperature gradient in the y -direction is much larger than that in the x -direction and hence only the thermophoretic velocity component which is normal to the surface is of importance (iii) the fluid is considered to be gray; absorbing-emitting radiation but non-scattering medium and the Rosseland approximation is used to describe the radioactive heat flux in the x -direction, (iv) the fluid property variation with temperature are limited to viscosity, (v) there exists a homogeneous n -th order chemical reaction between the fluid and species concentration, (vi) viscous dissipation and joule heating terms are neglected for low speed flows and, (v) the level of species concentration is very low so that the heat generated during chemical reaction can be neglected.

Since the plate is of infinite extent, all derivatives with respect to are supposed to be zero and hence under the usual Boussinesq and boundary-layer approximation, the governing equations for this problem can be written as follows:

$$\frac{\partial v}{\partial y} = 0 \quad (\text{continuity}), \quad (1)$$

$$\frac{\partial u}{\partial t} + v \frac{\partial u}{\partial y} = \frac{1}{\rho_\infty} \frac{\partial}{\partial y} \left(\mu \frac{\partial u}{\partial y} \right) + g\beta(T - T_\infty) \cos \alpha - \frac{\sigma B_0^2}{\rho_\infty} u \quad (\text{momentum}), \quad (2)$$

$$\frac{\partial T}{\partial t} + v \frac{\partial T}{\partial y} = \frac{\lambda_g}{\rho_\infty c_p} \frac{\partial^2 T}{\partial y^2} - \frac{1}{\rho_\infty c_p} \frac{\partial q_r}{\partial y} \quad (\text{energy}), \quad (3)$$

$$\frac{\partial C}{\partial t} + v \frac{\partial C}{\partial y} = D \frac{\partial^2 C}{\partial y^2} - \frac{\partial}{\partial y} (V_T C) - K_1 C^n \quad (\text{diffusion}), \quad (4)$$

where u, v are the velocity components in the x and y directions respectively, t is the time, μ is the fluid viscosity, g is the acceleration due to gravity, σ is the electrical conductivity,

ρ_∞ is the ambient density, β is the volumetric coefficient of thermal expansion, T, T_w and T_∞ are the temperature of the fluid inside the thermal boundary layer, the plate temperature and the fluid temperature in the free stream, respectively, while C, C_w and C_∞ are the corresponding concentrations, B_0 is the magnetic induction, λ_g is the thermal conductivity of the fluid, c_p is the specific heat at constant pressure, q_r is the radiative heat flux in the y -direction, D is the molecular diffusivity of the species concentration, V_T is the thermophoretic velocity, K_l is the chemical reaction parameter and n is the order of chemical reaction.

The initial and boundary conditions for the above problem are:

for $t \leq 0$:

$$u = v = 0, \quad T = T_\infty, \quad C = C_\infty \quad \text{for all } y,$$

for $t > 0$:

$$u = U_0, \quad v = \pm v(t), \quad T = T_w, \quad C = C_w = 0 \quad \text{at } y = 0, \quad (5a)$$

$$u = 0, \quad T = T_\infty, \quad C = C_\infty = 0 \quad \text{as } y \rightarrow \infty, \quad (5b)$$

where $v(t)$ is the time dependent suction/injection velocity at the porous plate.

The radiative heat flux under Rosseland approximation (see Sparrow and Cess [25], Brewster [26]) has the form

$$q_r = -\frac{4\sigma_1}{3k_1} \frac{\partial T^4}{\partial y}, \quad (6)$$

where σ_1 is the Stefan-Boltzmann constant and k_1 is the mean absorption coefficient.

We assume that the temperature difference within the flow are sufficiently small such that T^4 may be expressed as a linear function of temperature. This is accomplished by expanding T^4 in a Taylor series about T_∞ and neglecting higher-order terms, thus

$$T^4 \cong 4T_\infty^3 T - 3T_\infty^4. \quad (7)$$

Using (6) and (7) in equation (3) we have

$$\frac{\partial T}{\partial t} + v \frac{\partial T}{\partial y} = \frac{\lambda_g}{\rho c_p} \frac{\partial^2 T}{\partial Y^2} + \frac{16\sigma_1 T_\infty^3}{3\rho c_p k_1} \frac{\partial^2 T}{\partial y^2}. \quad (8)$$

In equation (4), the thermophoretic velocity V_T was given by Talbot et al. [27] as:

$$V_T = -k\nu \frac{\nabla T}{T_0} = -\frac{k\nu}{T_0} \frac{\partial T}{\partial y}, \quad (9)$$

where T_0 is some reference temperature, the value of $k\nu$ represents the thermophoretic diffusivity, and k is the thermophoretic coefficient which ranges in value from 0.2 to 1.2 as indicated by Batchelor and Shen [28] and is defined from the theory of Talbot et al. [27] by:

$$k = \frac{2C_s(\lambda_g/\lambda_p + C_t Kn)[1 + Kn(C_1 + C_2 e^{-C_3/Kn})]}{(1 + 3C_m Kn)(1 + 2\lambda_g/\lambda_p + 2C_t Kn)}, \quad (10)$$

where $C_1, C_2, C_3, C_m, C_s, C_t$ are constants, λ_g and λ_p are the thermal conductivities of the fluid and diffused particles, respectively and Kn is the Knudsen number.

A thermophoretic parameter τ can be defined (see Mills et al. [2] and Tsai [29]) as follows:

$$\tau = -\frac{k(T_w - T_\infty)}{T_0}. \quad (11)$$

Typical values of τ are 0.01, 0.05 and 0.1 corresponding to approximate values of $-k(T_w - T_\infty)$ equal to 3, 15 and 30 K for a reference temperature of $T_0 = 300$ K.

For a viscous fluid, Ling and Dybbs [30] suggested a viscosity dependence on the temperature T of the form

$$\mu = \frac{\mu_\infty}{[1 + \gamma(T - T_\infty)]}, \quad (12)$$

so that viscosity is an inverse linear function of temperature T .

Equation (12) can be rewritten as

$$\frac{1}{\mu} = A(T - T_r), \quad (13)$$

where

$$A = \frac{\gamma}{\mu_\infty} \quad \text{and} \quad T_r = T_\infty - \frac{1}{\gamma}. \quad (14)$$

In the above relations (14), both A and T_r are constants and their values depend on the reference state and γ , a thermal property of the fluid. In general, $A > 0$ for liquids, and $A < 0$ for gases. Typical values of γ and A for air are $\gamma = 0.026240$ and $A = -123.2$ (see Weast [31]).

To obtain local similarity solution in time of the problem under consideration, we introduce a time dependent length scale δ as

$$\delta = \delta(t). \quad (15)$$

In terms of this length scale, a convenient solution of the equation (1) is considered to be in the following form:

$$v = v(t) = -v_0 \frac{\nu}{\delta}, \quad (16)$$

where v_0 is the suction/injection parameter.

We now introduce the following dimensionless variables:

$$\eta = \frac{y}{\delta}, \quad u = U_0 f(\eta), \quad \theta(\eta) = \frac{T - T_\infty}{T_w - T_\infty}, \quad \phi(\eta) = \frac{C}{C_\infty}. \quad (17)$$

The dimensionless temperature θ can also be written as

$$\theta = \frac{T - T_r}{T_w - T_\infty} + \theta_r, \quad (18)$$

where

$$\theta_r = \frac{T_r - T_\infty}{T_w - T_\infty} = -\frac{1}{\gamma(T_w - T_\infty)} = \text{const}, \quad (19)$$

and its value is determined by the viscosity/temperature characteristics of the fluid under consideration and the operating temperature difference $\Delta T = T_w - T_\infty$.

Then introducing the relations (9), (12), (13), (16), (17) and (19) into the equations (2), (3) and (4), respectively, we then obtain the following ordinary differential equations:

$$f'' + \eta \left(\frac{\delta}{\nu} \frac{d\delta}{dt} \right) \left(\frac{\theta_r - \theta}{\theta_r} \right) f' + v_0 \left(\frac{\theta_r - \theta}{\theta_r} \right) f' + \frac{\theta'}{\theta_r - \theta} f' + Gr \left(\frac{\theta_r - \theta}{\theta_r} \right) \theta \cos \alpha - M \left(\frac{\theta_r - \theta}{\theta_r} \right) f = 0, \quad (20)$$

$$-\eta \left(\frac{\delta}{\nu} \frac{d\delta}{dt} \right) \theta' - v_0 \theta' = \left(\frac{3R + 4}{3RPr} \right) \theta'', \quad (21)$$

$$-\eta \left(\frac{\delta}{\nu} \frac{d\delta}{dt} \right) \phi' - v_0 \phi' = \frac{1}{Sc} \phi'' - \tau (\phi \theta'' + \phi' \theta') - K \phi^n, \quad (22)$$

where $Pr = \frac{\rho_\infty c_p \nu}{\lambda_g}$ is the Prandtl number, $Sc = \frac{\nu}{D}$ is the Schmidt number, $M = \frac{\sigma B_0^2 \delta^2}{\nu \rho_\infty}$ is the local magnetic field parameter, $Gr = \frac{g \beta (T_w - T_\infty) \delta^2}{\nu U_0}$ is the local Grashof number, $R = \frac{\lambda_g k_1}{4 \sigma_1 T_\infty^3}$ is the radiation parameter, and $K = \frac{K_1 \delta^2}{\nu}$ is the local chemical reaction parameter.

The corresponding boundary conditions for $t > 0$ are obtained as:

$$f = 1, \quad \theta = 1, \quad \phi = 0 \quad \text{at } \eta = 0, \quad (23a)$$

$$f = 0, \quad \theta = 0, \quad \phi = 1 \quad \text{as } \eta \rightarrow \infty. \quad (23b)$$

Now the equations (20)–(22) are locally similar except the term $\left(\frac{\delta}{\nu} \frac{d\delta}{dt} \right)$, where t appears explicitly. Thus the local similarity condition requires that the term $\left(\frac{\delta}{\nu} \frac{d\delta}{dt} \right)$ in the equations (20)–(22) must be a constant quantity.

Hence, following the works of Hasimoto [32], Sattar and Hossain [33], Alam et al. [34], Rahman and Sattar [35] one can try a class of solutions of the equations (20)–(22) by assuming that

$$\left(\frac{\delta}{\nu} \frac{d\delta}{dt} \right) = \lambda \quad (\text{a constant}). \quad (24)$$

Integrating (24) we have

$$\delta = \sqrt{2\lambda\nu t}, \quad (25)$$

where the constant of integration is determined through the condition that $\delta = 0$ when $t = 0$. We have considered the problem for small time. In this case normal velocity

in (16) will be large i.e., suction will be large, which can be applied to increase the lift of the airfoils. From (24) choosing $\lambda = 2$, the length scale $\delta(t) = 2\sqrt{\nu t}$ which exactly corresponds to the usual scaling factor for various unsteady boundary layer flows (Schlichting [36]). Since is a scaling factor as well as a similarity parameter, any value of λ in (24) would not change the nature of the solution except that the scale would be different.

Now introducing (24) (with $\lambda = 2$) in the equations (20)–(22) respectively, we obtain the following dimensionless non-linear ordinary differential equations which are locally similar in time but not explicitly time dependent.

$$f'' + (2\eta + v_0) \left(\frac{\theta_r - \theta}{\theta_r} \right) f' + \frac{\theta'}{\theta_r - \theta} f' + Gr \left(\frac{\theta_r - \theta}{\theta_r} \right) \theta \cos \alpha - M \left(\frac{\theta_r - \theta}{\theta_r} \right) f = 0, \quad (26)$$

$$\theta'' + (2\eta + v_0) \left(\frac{3RPr}{3R + 4} \right) \theta' = 0, \quad (27)$$

$$\phi'' + Sc(2\eta + v_0)\phi' - \tau Sc(\phi\theta'' + \phi'\theta') - ScK\phi^n = 0, \quad (28)$$

where primes denote differentiation with respect to similarity variable η .

3 Local skin-friction coefficient, local Nusselt number and local Stanton number

The physical quantities of most interest for the present problem are the local skin-friction coefficient (dimensionless wall shear stress), the local Nusselt number (rate of heat transfer) and the local Stanton number (rate of transfer of species concentration) which are defined respectively by the following relations:

$$Cf = \frac{\tau_w}{\rho U_0^2}, \quad Nu = \frac{\delta q_w}{\lambda_g (T_w - T_\infty)} \quad \text{and} \quad St = -\frac{J_s}{U_0 C_\infty}. \quad (29)$$

Now the wall shear stress on the surface τ_w , rate of heat transfer q_w and rate of transfer of species concentration J_s are given by

$$\tau_w = \left[\mu \frac{\partial u}{\partial y} \right]_{y=0}, \quad (30a)$$

$$q_w = -\lambda_g \left(\frac{\partial T}{\partial y} \right)_{y=0} - \frac{4\sigma}{3k_1} \left(\frac{\partial T}{\partial y} \right)_{y=0}, \quad (30b)$$

$$J_s = -D \left[\frac{\partial C}{\partial y} \right]_{y=0}. \quad (30c)$$

Now using equation (7) we have from (30b)

$$\begin{aligned}
 q_w &= -\lambda_g \left(\frac{\partial T}{\partial y} \right)_{y=0} - \frac{16\sigma_1 T_\infty^3}{3k_1} \left(\frac{\partial T}{\partial y} \right)_{y=0} \\
 &= -\frac{\lambda_g \Delta T}{\delta} \theta'(0) - \frac{16\sigma_1 T_\infty^3 \Delta T}{3k_1 \delta} \theta'(0) \\
 &= -\frac{\lambda_g \Delta T}{\delta} \left(1 + \frac{4}{3R} \right) \theta'(0).
 \end{aligned} \tag{31}$$

Using (12), (17), (30) and (31) the quantities of (29) can be written as follows:

$$\begin{aligned}
 CfRe &= \frac{\theta_r}{\theta_r - 1} f'(0), \quad Nu = -\left(1 + \frac{4}{3R} \right) \theta'(0), \\
 StScRe &= \phi'(0),
 \end{aligned} \tag{32}$$

where $Re = \frac{U_0 \delta}{\nu}$ is the local Reynolds number.

4 Method of numerical solution

The system of non-linear and locally similar ordinary differential equations (26)–(28) together with the boundary conditions (23) have been solved numerically by using Nachtsheim-Swigert shooting iteration technique [37] along with sixth order Runge-Kutta integration scheme. The detailed discussion of the method can be found in our earlier paper Alam et al. [34].

Thus adopting this numerical technique, a computer program was set up for the solutions of the governing non-linear partial differential equations of our problem where the integration technique was adopted as a sixth-order Runge-Kutta method of integration. Various groups of the parameters $v_0, \theta_r, R, Pr, Sc, M, Gr, \tau, K, n$ and α were considered in different phases. In all the computations the step size $\Delta\eta = 0.01$ was selected that satisfied a convergence criterion of 10^{-6} in almost all of different phases mentioned above. The value of η_∞ was found to each iteration loop by the statement $\eta_\infty = \eta_\infty + \Delta\eta$. The maximum value of η_∞ , for each group of parameters, has been obtained when the value of the unknown boundary conditions at $\eta = 0$ does not change in the successful loop with an error less than 10^{-6} .

Care has been taken to see the effects of step size ($\Delta\eta$) on the integration procedure. For our system we ran the code with three different step sizes as $\Delta\eta = 0.01$, $\Delta\eta = 0.006$, $\Delta\eta = 0.001$ and in each case we found excellent agreement among them. Figs. 1(a)–(c) depicts respectively the dimensionless velocity, temperature and concentration profiles for different step sizes. These figures show that step size of $\Delta\eta = 0.01$ is sufficient getting a convergent solution.

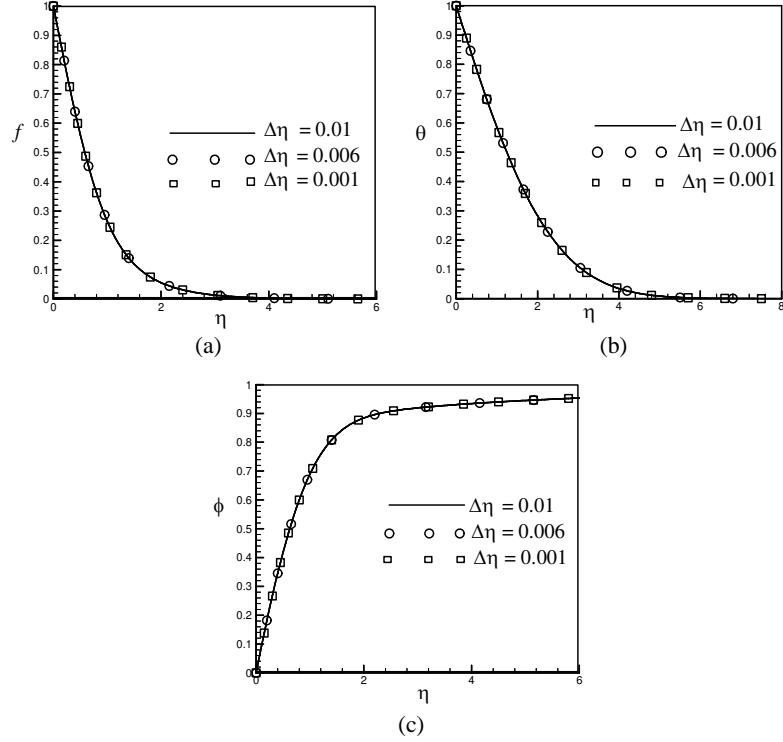


Fig. 1. (a) velocity, (b) temperature and (c) concentration profiles for different step size.

5 Results and discussion

For the purpose of discussing the effects of various parameters on the flow behaviour near the plate, numerical calculations have been carried out for different values of α , M , v_0 , θ_r , R , Sc , τ , K and n for a fixed value of Gr and Pr . Due to free convection problem, positive large value of $Gr = 6$ are taken which corresponds to a cooling problem and is generally encountered in nuclear engineering in connection with cooling of reactor. Throughout the study Prandtl number is kept constant at 0.7 which represents air at 293 K and 1 atmosphere of pressure. It is important to note that the viscosity/temperature parameter θ_r is negative for liquids and positive for gases when $(T_w - T_\infty)$ is positive. The values of θ_r (for air $\theta_r > 0$) are chosen to be 2, 4 and 6. The chemical reaction parameter K can be adjusted to meet the circumstances if one takes (i) $K > 0$ for destructive reaction, (ii) $K = 0$ for the generative reaction, and (iii) for no reaction. The default values of the other physical parameters are $\alpha = 30^\circ$, $M = 0.4$, $\theta_r = 2.0$, $v_0 = 0.5$, $R = 0.3$, $Sc = 0.6$, $\tau = 0.1$, $K = 0.1$ and $n = 1.0$ unless otherwise specified.

Fig. 2 shows the effect of angle of inclination to the vertical direction on the velocity profiles. From this figure we observe that the velocity is decreased by increasing the

angle of inclination. The fact is that as the angle of inclination increases the effect of the buoyancy force due to thermal diffusion decreases by a factor of $\cos \alpha$. Consequently the driving force to the fluid decreases as a result velocity profiles decrease.

The effect of the magnetic field parameter M on the velocity profiles is displayed in Fig. 3. The presence of a magnetic field normal to the flow in an electrically conducting fluid introduces a Lorentz force which acts against the flow. This resistive force tends to slow down the flow and hence the fluid velocity decreases with the increase of the magnetic field parameter as observed in Fig. 3. It is also seen that thickness of the thermal boundary layer decreases with the increase of the magnetic field parameter.

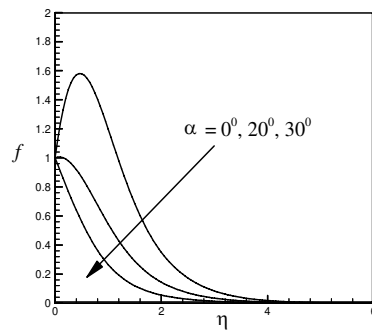


Fig. 2. Velocity profiles for different values of α .

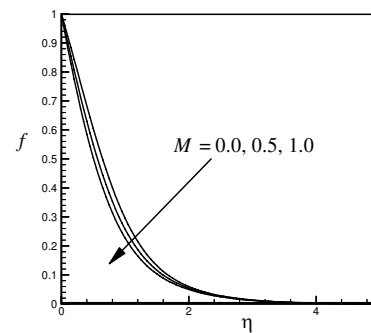


Fig. 3. Velocity profiles for different values of M .

The effect of the viscosity/temperature parameter θ_r on the velocity and temperature profiles is presented in Figs. 4(a), (b) respectively. From these figures we observe that velocity profiles increase whereas temperature profiles decrease with the increasing values of θ_r . This is due to the fact that increase of the viscosity/temperature parameter θ_r makes decrease of the thermal boundary layer thickness, which results in decrease of the temperature boundary layer.

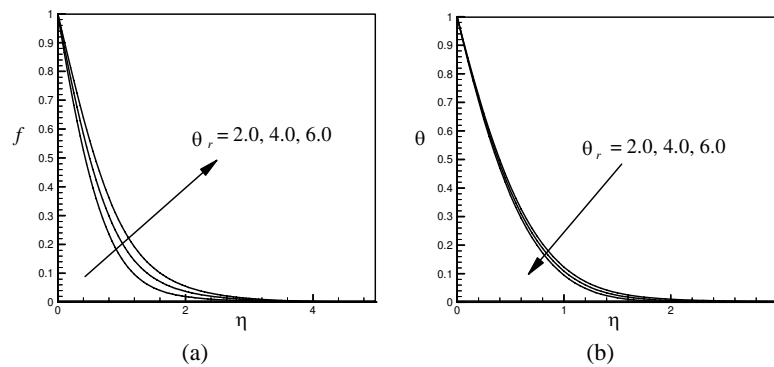


Fig. 4. (a) Velocity and (b) temperature profiles for different values of θ_r .

Figs 5(a),(b) respectively represent the dimensionless velocity and temperature profiles for different values of radiation parameter R . It is seen from these figures that both the velocity and temperature profiles decrease with the increase of the radiation parameter.

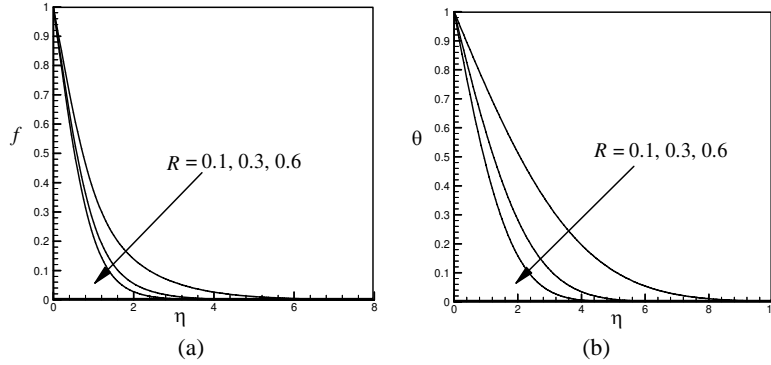


Fig. 5. (a) Velocity and (b) temperature profiles for different values of R .

Fig. 6 shows the dimensionless concentration profiles for different values of the Schmidt number Sc . It is clear from this figure that the concentration boundary layer thickness decreases as the Schmidt number Sc increases and this is the analogous to the effect of increasing the Prandtl number on the thickness of a thermal boundary layer.

The effect of thermophoretic parameter τ on the concentration field is shown in Fig. 7. From this figure we see that the effect of increasing the thermophoretic parameter τ is limited to increasing slightly the wall slope of the concentration profiles for $\eta < 0.80$ but decreasing the concentration for values of $\eta > 0.80$.

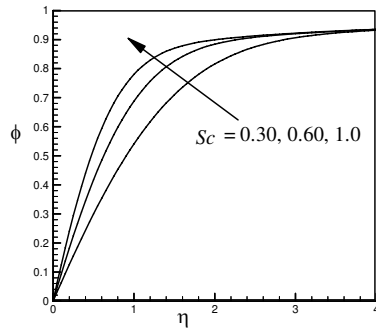


Fig. 6. Concentration profiles for different values of Sc .

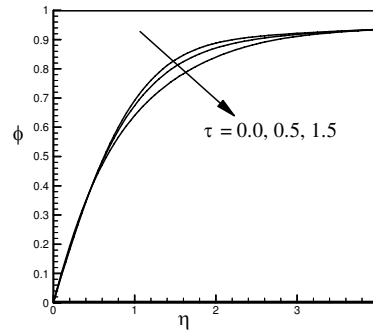


Fig. 7. Concentration profiles for different values of τ .

The effect of chemical reaction parameter K on the concentration field is shown in Fig. 8. From this figure we see that the concentration increases during the generative

reaction ($K < 0$) and decreases in the destructive reaction ($K > 0$). This shows that diffusion rate can be tremendously altered by chemical reactions. From this figure we also observe that for generative reaction, concentration profile overshoots within the boundary layer. This may be attributed to the fact that decreasing values of K implies more interaction of species concentration within the boundary layer.

The effect of n (order of chemical reaction) on the concentration distributions is presented in Fig. 9 for destructive chemical reaction ($K > 0$). From this figure we see that the concentration profiles increase with the increasing values of n .

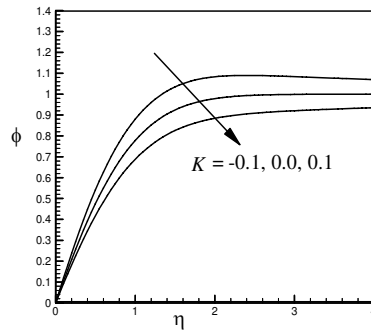


Fig. 8. Concentration profiles for different values of K .

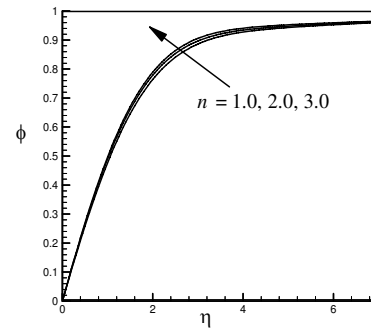


Fig. 9. Concentration profiles for different values of n .

Table 1 represents the effects of v_0 and θ_r on the local skin-friction coefficient (Cf), the local Nusselt number (Nu) and the local Stanton number (St). From this table we see that the local skin-friction coefficient decreases whereas both the local Nusselt number as well as the local Stanton number increases for wall fluid suction ($v_0 > 0$). But imposition of wall fluid injection ($v_0 < 0$) produces the opposite effects compared to the case of wall fluid suction. It is also seen from this table that both the local skin-friction coefficient (Cf) and the local Nusselt number (Nu) increases with the increasing values of θ_r but the local Stanton number (St) is not sensitive to change as the viscosity/temperature parameter.

Table 1. Effects of v_0 and θ_r on Cf , Nu and St

v_0	θ_r	Cf	Nu	St
-0.5	2.0	-0.4952308	0.3678345	0.3845293
0.0	2.0	-1.0062674	0.4057341	0.7453271
0.5	2.0	-1.3813645	0.4464034	0.9481058
1.0	2.0	-1.7408219	0.4998574	1.1550713
1.5	2.0	-2.1085590	0.5448530	1.3549843
1.5	4.0	-1.8742142	0.5639641	1.3549843
1.5	6.0	-1.6398694	0.5849254	1.3549843

Table 2 shows the effects of Pr and R on the local skin-friction coefficient (Cf), the local Nusselt number (Nu), and the local Stanton number (St). From this table we

see that as the radiation parameter R increases, the local skin-friction coefficient and the local Stanton number decrease while the Nusselt number increases for liquid metals ($Pr = 0.05$), air ($Pr = 0.70$) as well as for water ($Pr = 7.0$).

Table 2. Effects of Pr and R on Cf , Nu and St

Pr	R	Cf	Nu	St
0.05	0.1	-0.2908024	0.0813754	0.9428877
0.05	0.3	-0.4087336	0.1139205	0.9421206
0.05	0.6	-0.5051421	0.1460564	0.9413075
0.70	0.1	-0.7428116	0.2651156	0.9483914
0.70	0.3	-0.9372340	0.4464034	0.9475822
0.70	0.6	-1.0360335	0.5969869	0.9458703
7.00	0.1	-1.1755652	0.9503326	0.9496639
7.00	0.3	-1.3163509	1.7149534	0.9489905
7.00	0.6	-1.3793518	2.4109572	0.9475907

The effects of Schmidt number Sc and thermophoretic parameter τ on the local Stanton number (St) are shown in Table 3. It is observed from this table that the local Stanton number increases as St or τ increases.

Finally in Table 4, the effects of the chemical reaction parameter and the order of the chemical reaction on the local Stanton number (St) are presented. It is observed from this table that the local Stanton number decreases with the increase of K for a destructive reaction ($K > 0$) and increases with the decrease of K for a generative reaction ($K < 0$). It is also found from this table that the local Stanton number increases with the increasing values of n for both destructive as well as generative reaction.

Table 3. Effects of Sc and τ on St

Sc	τ	St
0.30	0.5	0.6531895
0.30	1.0	0.6687925
0.30	1.5	0.6841851
0.60	0.5	0.9831672
0.60	1.0	1.0249262
0.60	1.5	1.0659454
1.00	0.5	1.3544947
1.00	1.0	1.4376140
1.00	1.5	1.5189339

Table 4. Effects of K and n on St

K	n	St
-0.2	1.0	1.4187066
0.0	1.0	1.0822959
0.1	1.0	0.9485822
-0.2	2.0	1.4483635
0.0	2.0	1.0822959
0.1	2.0	0.9746693
-0.2	3.0	1.5134239
0.0	3.0	1.0822959
0.1	3.0	0.9947767

6 Conclusions

This paper deals with the effects of variable viscosity, thermophoresis as well as n -th order chemical reaction on an unsteady MHD free convective heat and mass transfer flow past an impulsively started infinite inclined porous plate in the presence of thermal radiation. The fluid viscosity has been assumed to vary as an inverse linear function

of the temperature. By introducing a time dependent length scale as well as similarity transformation, the governing non-linear partial differential equations have been transformed into a system of non-dimensional ordinary differential equations which are locally similar and solved them numerically using shooting method. From the present numerical investigation we may conclude the followings:

1. Imposition of wall fluid suction ($v_0 > 0$) decreases the local skin-friction coefficient whereas increases the local Nusselt number as well as the local Stanton number along the surface of the plate. But imposition of wall fluid injection ($v_0 < 0$) produces the opposite effects compared to the wall fluid suction.
2. Viscosity/temperature parameter increases viscous drag as well as rate of heat transfer.
3. Radiation significantly controls the velocity as well as thermal boundary layers.
4. Chemical reaction significantly alters the diffusion rate.
5. Higher order chemical reaction induces the concentration of the particles for a destructive reaction and reduces for a generative reaction.

Acknowledgement

We would like to thank the anonymous referee for his very constructive and expertise comments that helped to further improvement of the paper. One of the authors M. S. Alam is grateful to “Prime Minister’s Fund for Higher Studies” – The People’s Republic of Bangladesh for funding through a research studentship.

References

1. K. L. Walker, G. M. Homsy, F. T. Geying, Thermophoretic deposition of small particles in laminar tube, *J. Colloid Interf. Sci.*, **69**, pp. 138–147, 1979.
2. A. F. Mills, X. Hang, F. Ayazi, The effect of wall suction and thermophoresis on aerosol-particle deposition from a laminar boundary layer on a flat plate, *Int. J. Heat Mass Tran.*, **27**, pp. 1110–1113, 1984.
3. Y. Ye, D. Y. H. Pui, B. Y. H. Liu, S. Opiolka, S. Blumhorst, H. Fissan, Thermophoretic effect of particle deposition on a free standing semiconductor wafer in a clean room, *J. Aerosol Sci.*, **22**(1), pp. 63–72, 1991.
4. D. G. Thakurta, M. Chen, J. B. Mclaughlin, K. Kontomaris, Thermophoretic deposition of small particles in a direct numerical simulation of turbulent channel flow, *Int. J. Heat Mass Tran.*, **41**, pp. 4167–4182, 1998.
5. P. Han, T. Yoshida, Numerical investigation of thermophoretic effects on cluster transport during thermal plasma deposition process, *J. Appl. Phys.*, **91**(4), pp. 1814–1818, 2002.

6. M. S. Alam, M. M. Rahman, M. A. Sattar, Similarity solutions for hydromagnetic free convective heat and mass transfer flow along a semi-infinite permeable inclined flat plate with heat generation and thermophoresis, *Nonlinear Anal. Model. Control*, **12**(4), pp. 433–445, 2007.
7. S. J. Yoa, S. S. Kim, J. S. Lee, Thermophoresis of highly absorbing emitting particles in laminar tube flow, *Int. J. Heat Fluid Fl.*, **11**(1), pp. 98–104, 1990.
8. Y. M. Sohn, S. W. Beak, D. Y. Kim, Thermophoresis of particles in gas-particle two-phase flow with radiation effect, *Numerical Heat Tr. A-Appl.*, **41**, pp. 165–181, 2002.
9. M. K. Akbar, S. M. Ghiaasiaan, Radiation heat transfer and soot thermophoresis in laminar tube flow, *Numerical Heat Tr. A-Appl.*, **47**(7), pp. 653–670, 2005.
10. M. S. Alam, M. M. Rahman, M. A. Sattar, Effects of variable suction and thermophoresis on steady mhd combined free-forced convective heat and mass transfer flow over a semi-infinite permeable inclined plate in the presence of thermal radiation, *Int. J. Therm. Sci.*, **47**(6), pp. 758–765, 2008.
11. R. Cortell, Viscous flow and heat transfer over a nonlinearly stretching sheet, *Appl. Math. Comput.*, **184**(2), pp. 864–873, 2007.
12. R. Cortell, Effects of viscous dissipation and radiation on the thermal boundary layer over a nonlinearly stretching sheet, *Phys. Lett. A*, **372**(5), pp. 631–636, 2008.
13. R. Cortell, Similarity solutions for flow and heat transfer of a quiescent fluid over a nonlinearly stretching sheet, *J. Mater. Process. Tech.*, **203**(1–3), pp. 176–183, 2008.
14. P. L. Chambre, J. D. Young, On the diffusion of a chemically reactive species in a laminar boundary layer flow, *Phys. Fluids*, **1**, pp. 48–54, 1958.
15. U. N. Das, R. K. Deka, V. M. Soundalgekar, Effects of mass transfer on flow past an impulsively started infinite vertical plate with constant heat flux and chemical reaction, *Forsch. Ingenieurwes.*, **60**, pp. 284–287, 1994.
16. S. P. Anjalidevi, R. Kandasamy, Effects of chemical reaction heat and mass transfer on MHD flow past a semi-infinite plate, *Z. Angew. Math. Mech.*, **80**, pp. 697–701, 2000.
17. R. Muthucumaraswamy, P. Ganesan, First order chemical reaction on flow past an impulsively started vertical plate with uniform heat and mass flux, *Acta Mech.*, **147**, pp. 45–57, 2001.
18. A. Raptis, C. Perdakis, Viscous flow over a non-linearly stretching sheet in the presence of a chemical reaction and magnetic field, *Int. J. Nonlinear Mech.*, **41**, pp. 527–529, 2006.
19. R. Cortell, MHD flow and mass transfer of an electrically conducting fluid of second grade in a porous medium over a stretching sheet with chemically reactive species, *Chem. Eng. Process.*, **46**, pp. 721–728, 2007.
20. R. Cortell, Toward an understanding of the motion and mass transfer with chemically reactive species for two classes of viscoelastic fluid over a porous stretching sheet, *Chemical Engineering and Processing: Process Intensification*, **46**, pp. 982–989, 2007.

21. M. S. Alam, M. M. Rahman, M. A. Sattar, Effects of thermophoresis and chemical reaction on unsteady hydromagnetic free convection and mass transfer flow past an impulsively started infinite inclined porous plate in the presence of heat generation/absorption, *Thammasat Int. J. Sci. Tech.*, **12**(3), 44–52, 2007.
22. N. G. Kafousias, E. W. Williams, Thermal-diffusion and Diffusion-thermo effects on mixed free-forced convective and mass transfer boundary layer flow with temperature dependent viscosity, *Int. J. Eng. Sci.*, **33**(9), pp. 1369–1384, 1995.
23. M. A. Seddeek, The effect of variable viscosity on hydromagnetic flow and heat transfer past a continuously porous boundary with radiation, *Int. Commun. Heat Mass*, **27**, pp. 1037–1048, 2000.
24. M. M. Molla, M. A. Hossain, Effects of chemical reaction, heat and mass diffusion in natural convection flow from an isothermal sphere with temperature dependent viscosity, *Int. J. Computer-Aided Engineering and Software*, **23**(7), pp. 840–857, 2006.
25. E. M. Sparrow, R. D. Cess, *Radiation Heat Transfer*, Augmented ed., Hemisphere Publishing Corporation, Washington D. C., 1978.
26. M. Q. Brewster, *Thermal Radiative Transfer and Properties*, John Wiley and Sons, New York, 1992.
27. L. Talbot, R. K. Cheng, A. W. Schefer, D. R. Wills, Thermophoresis of particles in a heated boundary layer, *J. Fluid Mech.*, **101**, pp. 737–758, 1980.
28. G. K. Batchelor, C. Shen, Thermophoretic deposition of particles in gas flowing over cold surface, *J. Colloid Interf. Sci.*, **107**, pp. 21–37, 1985.
29. R. Tsai, A simple approach for evaluating the effect of wall suction and thermophoresis on aerosol particle deposition from a laminar flow over a flat plate, *Int. Commun. Heat Mass*, **26**, pp. 249–257, 1999.
30. J. X. Ling, A. Dybbs, *Forced convection over a Flat Plate Submersed in a Porous Medium, Variable Viscosity case*, ASME Paper 87-WA/HT-23, New York, 1987.
31. R. C. Weast, *Handbook of Chemistry and Physics*, 71th ed., C. R. C. Press, Boca Raton, 1990.
32. H. Hasimoto, Boundary layer growth on a flat plate with suction or injection, *J. Phys. Soc. Jpn.*, **12**, pp. 68–72, 1956.
33. M. A. Sattar, M. M. Hossain, Unsteady hydromagnetic free convection flow with Hall current and mass transfer along an accelerated porous plate with time dependent temperature and concentration, *Can. J. Phys.*, **70**, pp. 369–374, 1992.
34. M. S. Alam, M. M. Rahman, M. A. Samad, Numerical study of the combined free-forced convection and mass transfer flow past a vertical porous plate in a porous medium with heat generation and thermal diffusion, *Nonlinear Anal. Model. Control*, **11**(4), pp. 331–343, 2006.
35. M. M. Rahman, M. A. Sattar, Transient convective flow of micropolar fluid past a continuously moving vertical porous plate in the presence of radiation, *Int. J. Appl. Mech. Eng.*, **12**(2), pp. 497–513, 2007.

36. H. Schlichting, *Boundary Layer Theory*, 6th ed., McGraw-Hill, New York, 1968.
37. P. R. Nachtsheim, P. Swigert, *Satisfaction of the asymptotic boundary conditions in numerical solution of the system of non-linear equations of boundary layer type*, NASA TND-3004, 1965.